JOURNAL OF Applied Polymer SCIENCE

Morphology and Dielectric Relaxation Spectroscopy of Ternary Polymer Blends of Polyamide6, Polypropylene, and Acrylonitrile Butadiene Styrene Co-polymer: Influence of Compatibilizer and Multiwall Carbon Nanotubes

Biswajit Panda, Arup R. Bhattacharyya, Ajit R. Kulkarni
Department of Metallurgical Engineering and Materials Science, Indian Institute of Technology Bombay, Powai, Mumbai-400076, India
Correspondence to: A. R. Bhattacharyya (E-mail: arupranjan@iitb.ac.in)

ABSTRACT: Morphological investigation was carried out with melt-mixed ternary polymer blends of polyamide6 (PA6), polypropylene (PP) and acrylonitrile butadiene styrene copolymer (ABS) in the presence of compatibilizer and multiwall carbon nanotubes (MWNTs). 80/10/10 (wt/wt/wt) PA6/PP/ABS and 80/10/10 (wt/wt/wt) PP/PA6/ABS blends exhibited "core-shell" morphology, whereas 80/10/10 (wt/wt/wt) ABS/PP/PA6 blends exhibited "separately dispersed" phase morphology. The type of phase morphology was unaltered in the presence of either compatibilizer or MWNTs in the respective ternary polymer blends. The morphological refinement in the presence of compatibilizer was explained on the basis of melt-interfacial reaction. In contrast, the refinement in the dispersed droplets in the presence of MWNTs was due to the localization of MWNTs in the specific phase. Dynamic relaxation spectroscopic analysis indicated an increase in the relaxation time of PA6 chain in the presence of compatibilizer in the corresponding ternary blends. The variation in the relaxation time was dependent on the efficiency of the compatibilizer. The variation in the relaxation time for PA6 in the presence of 1 wt% MWNTs in the respective ternary blends also followed a similar trend; however, the extent of mobility of PA6 phase was influenced by the state of dispersion of MWNTs in the corresponding blends. © 2012 Wiley Periodicals, Inc. J. Appl. Polym. Sci. 000: 000–000, 2012

KEYWORDS: ternary polymer blends; "core-shell" morphology; dielectric relaxation

Received 17 November 2010; accepted 17 May 2012; published online
DOI: 10.1002/app.38074

INTRODUCTION

To develop a polymeric material with desired mechanical properties, melt-blending of two or more polymers has been found to be the most common and commercially adopted techniques.[1–6] Morphology, which develops during melt-mixing, is one of the most important factors in deciding the final property of the blends. Three major factors are reported to influence the phase morphology development in immiscible multicomponent polymer blends: interfacial tension of the constituent polymers,[7] melt-viscosity,[8] and melt-elasticity of the polymer components.[9] Hobbs et al.[7] have explained the development of phase morphology in the ternary polymer blends on the basis of spreading coefficient by modifying the Harkin's equation, in which two dissimilar phases are dispersed in the third phase (matrix). According to the signs of the spreading coefficient, for a given matrix, four types of morphologies could be predicted.[10]

A majority of the binary or ternary polymer blends are immiscible and incompatible in nature, which exhibits coarse and unstable phase morphology. Compatibilization technique is generally adopted in order to achieve finer morphology with adequate interfacial adhesion which leads to superior mechanical properties.[11]

In case of ternary polymer blends, the interfacial tension of the constituent components primarily decides whether the dispersed phase may exhibit "core-shell" type morphology or a "separately dispersed" phase morphology, which may lead to a variation in the ultimate mechanical properties. However, ternary polymer blends with "core-shell" morphology may not always be a substitute for compatibilized blends of the three component polymer blend. Hence, it is necessary to use compatibilizer to enhance the interfacial interaction between the phases. The technique of reactive compatibilization is a very unique route to achieve multiphase polymer blends with finer morphology.[12] Ha et al.[13] used chlorinated polyethylene (CPE) and ethylene polypropylene rubber (EPR) as dual compatibilizer to compatibilize 80/10/10 (wt/wt/wt) HDPE/PP/PVC ternary polymer blends, which resulted in significant improvement in impact strength. Fang et al.[14] showed the influence of the addition of three

compatibilizers e.g., CPE, ethylene-propylene-diene monomer (EPDM), styrene-butadiene-styrene (SBS) on the phase morphology of 70/10/10/10 (wt/wt/wt/wt) LDPE/PVC/PP/PS immiscible quaternary polymer blends. Omonov et al.[15] compatibilized ternary polymer blends of PA6/PP/PS using two reactive modifier viz. polypropylene grafted maleic anhydride (PP-*g*-MA) and styrene maleic anhydride (SMA). Wang et al.[16] reported that the addition of a single compatibilizer (viz. polypropylene grafted maleic anhydride-*co*-styrene [PP-*g*-(MA-co-St)] was more effective than either PP-*g*-MA or polypropylene grafted styrene (PP-*g*-St) or their mixture in PP/PA6/PS ternary blend.

Dielectric relaxation spectroscopy has been used in general to measure long and short range motion of polymer chains or macromolecular fragments as a function of temperature and frequency. Urman et al.[17] have shown that polyamide6 (PA6) exhibits three relaxation peaks; low temperature γ-relaxation, β-relaxation and higher temperature α-relaxation. Further, the presence of phosphate glass (Pglass) in PA6 was observed to accelerate both the α- and β-relaxation of PA6; however, the γ-relaxation was found to be unaffected. It has also been reported that the relaxation time of PA6 chain increases in the presence of nanofiller.[18] Logakis et al.[19] have studied the influence of multiwall carbon nanotubes (MWNTs) on the chain relaxation behavior of PA6. Further, it has been observed that the short range motion of PA6 chains remains unaffected in the presence of compatibilizer (PP-*g*-MA) in PP/PA6 binary blend.[20] George et al.[21] have studied the effect of blend ratio, filler addition (viz. carbon black, cork) and the dynamic vulcanization on the dielectric properties of i-PP/ acrylonitrile butadiene rubber (NBR) blends.

To understand the development of phase morphology in a ternary polymer blends, a model blend composition (80/10/10, wt/wt/wt) has been selected comprising of the following constituent polymers, viz., PA6, PP and acrylonitrile butadiene styrene copolymer (ABS). The matrix phase was interchanged between the three polymers in 80/10/10 (wt/wt/wt) ternary polymer blends in order to achieve various phase morphologies like "core-shell" and "separately dispersed" structure. Reactive compatibilization (with the addition of PP-*g*-MA and SMA) has been carried out to achieve finer morphology of the respective ternary blends. MWNTs were introduced to alter the phase morphology of these blends with an expectation that it would act as a compatibilizer. Dielectric relaxation spectroscopy has been used to understand the relaxation behavior of the PA6 phase in the presence of either compatibilizer or MWNTs. FTIR spectroscopic analysis has been utilized to investigate the melt-interfacial reaction in the presence of the reactive compatibilizer.

EXPERIMENTAL

Materials

Polyamide 6 (PA6, zero shear viscosity $\sim$ 180 Pa.s at 260°C) was obtained from GSFC, Gujarat, India (Gujlon M28RC, relative viscosity 2.8, M_v is 38,642 in 85% formic acid). Polypropylene (PP, zero shear viscosity $\sim$ 385 Pa.s at 260°C) was obtained from Reliance Industries, Mumbai, India (H200MA with melt flow index (MFI) of 23 g/10 min @ 230°C with a load of 2.16 kg). Acrylonitrile-butadiene-styrene (ABS) copolymer (Absolac-120, composition: acrylonitrile 24 wt %, styrene 59.5 wt % and rubber content 16.5 wt %, melt-viscosity at 0.01 rad/s $\sim 10^4$ Pa.s at 260°C) was procured from Bayer India Styrene-maleic anhydride copolymer (SMA) with 8% MA content (Dylark 232) was supplied by Nova Chemicals, USA. Polypropylene grafted maleic anhydride (PP-*g*-MA, P405 with MFI of 14 g/10 min @ 190°C with a load of 2.16 kg) was obtained from Plus Polymer, New Delhi, India with MA content of 0.9%. CCVD (catalytic carbon vapor deposition) synthesized purified multiwall carbon nanotubes (MWNTs) were obtained from Nanocyl CA, Belgium (NC-3100, average diameter: 9.5 nm and average length: 1.5 μm, purity>95%, as per manufacturer specifications).

Table I. Sample Codes with Their Compositions

Sample code	PA6 (wt %)	PP (wt %)	ABS (wt %)	SMA8 (wt %)	PP-*g*-MA (wt %)	MWNTs (wt %)
8N1P1A	80	10	10	0	0	0
8N1P1A2S	78.4	9.8	9.8	2	0	0
8N1P1A2P	78.4	9.8	9.8	0	2	0
8N1P1A2S2P	76.8	9.6	9.6	2	2	0
8N1P1A1T	79.2	9.9	9.9	0	0	1
8N1P1A2T	78.4	9.8	9.8	0	0	2
8P1N1A	10	80	10	0	0	0
8P1N1A 2S	9.8	78.4	9.8	2	0	0
8P1N1A 2P	9.8	78.4	9.8	0	2	0
8P1N1A2S2P	9.6	76.8	9.6	2	2	0
8P1N1A1T	9.9	79.2	9.9	0	0	1
8P1N1A2T	9.8	78.4	9.8	0	0	2
8A1P1N	10	10	80	0	0	0
8A1P1N2S	9.8	9.8	78.4	2	0	0
8A1P1N2P	9.8	9.8	78.4	0	2	0
8A1P1N2S2P	9.6	9.6	76.8	2	2	0
8A1P1N1T	9.9	9.9	79.2	0	0	1
8A1P1N2T	9.8	9.8	78.4	0	0	2

Blend Preparation

Ternary polymer blends of PA6, PP, and ABS were prepared by melt-mixing in a conical twin-screw microcompounder (Micro 5, DSM Research, Netherlands) at 260°C with a rotational speed of 150 rpm for 15 min. Blend compositions with their sample codes are mentioned in Table I. All the blend components were dried in a vacuum oven at 80°C for 24 h. Uncompatibilized and compatibilized ternary blends were prepared by following the simultaneous mixing protocol. However, MWNTs-based compositions were made by two-step mixing protocol, wherein; MWNTs were premixed for 10 min with the respective matrix polymer followed by the addition of the minor components for another 5 min (sequential mixing). Melt-mixing was performed under nitrogen atmosphere in order to prevent any oxidative degradation.

Injection-molded samples (according to ASTM D 638, Type V, thickness: 3 mm, length: 60 mm, parallel length: 12 mm) were

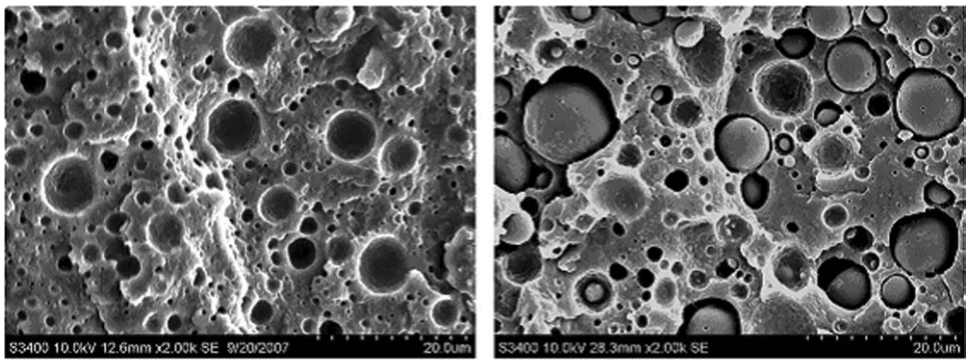

Figure 1. SEM micrographs of cryo-fractured and etched surfaces of 80/10/10 (wt/wt/wt) PA6/PP/ABS ternary polymer blends (a) etched with hot xylene (b) etched with THF.

prepared using mini injection-molding machine (DSM Research, Netherlands). The injection-molding parameters maintained for all the compositions were- injection pressure 3 bar, melt temperature 260°C, mold temperature 60°C, holding time 60 s and cooling time 2–3 min.

Characterization

Scanning Electron Microscopy. Scanning electron microscopy (SEM) was performed using Hitachi S3400N with gold sputtering on the etched surface. The extruded strands were cryo-fractured in liquid nitrogen and were selectively etched in the respective solvents (THF for ABS, hot xylene for PP and formic acid for PA6). Morphological investigation has also been carried out with the injection-molded sample, which was compared with the extrudate sample of identical composition. It has been observed (not shown here) that the morphology of the ternary blends did not vary significantly in the injection-molded sample (of the "core") due to further processing after melt-mixing, especially in the case of compatibilized and MWNTs incorporated compositions.

To evaluate the number average diameter (D_n) and weight average diameter (D_w) of the dispersed phase, ~ 200 droplets were analyzed using image analysis software (Olysia M3) for the respective ternary polymer blends and also for blends with MWNTs D_n and D_w of the dispersed droplets were calculated using the following equations:

$$D_n = (\sum n_i d_i)/(\sum n_i) \quad (1)$$

$$D_w = (\sum n_i d_i^2)/(\sum n_i d_i) \quad (2)$$

where, n_i indicates the number of droplets having d_i as their diameter.

Fourier Transform Infrared Spectroscopy. The measurements are carried out using the Vertex 80, Bruker FTIR equipment. The scanning range of the equipment is from 4000 cm^{-1}–400 cm^{-1}, with the spectral resolution of 4 cm^{-1}. The number of scans maintained while carrying out the spectroscopic measurement is kept as 32 scans. The powdered samples of the compatibilized blends were ground with KBr to prepare the pellets for the measurement. The powders were dried at 80°C for 24 h under vacuum.

Dielectric Relaxation Spectroscopy. Dielectric relaxation spectroscopic measurements were carried out with the injection-molded sample in the frequency range of 10^{-2}–10^{6} Hz and in the temperature range of −20°C to 120°C using Novocontrol alpha high-resolution analyzer. Silver paste was applied on both sides of the sample to ensure good electrical contact between the sample surface and the gold-plated capacitor plates. Relaxation time (τ) was estimated from the maximum peak (f_{max}) of dielectric loss modulus (M'') versus frequency plot, $\tau = (2\pi f_{max})^{-1}$.[22]

RESULTS AND DISCUSSION

Phase Morphology of 80/10/10 (wt/wt/wt) PA6/PP/ABS Ternary Polymer Blends

Phase morphology of 80/10/10 (wt/wt/wt) PA6/PP/ABS ternary polymer blends is presented in Figure 1, which shows "core-shell" morphological feature in the PA6 matrix. PP phase forms the "core" and the ABS phase forms the "shell" of the dispersed droplet. A similar type of morphology has been observed by Valera et al.[23] in case of 80/5/15 (wt/wt/wt) PMMA/PP/PS ternary polymer blends in which PP and PS phases are reported to form "core" and "shell" respectively in the PMMA matrix. Morphological analysis reveals a wide distribution of domain size of PP droplets, which indicates the incompatible nature of the ternary blends. D_n and D_w of the PP droplets in the various ternary blends are provided in Table II.

Table II. Average Droplet Size of PP Phase in 80/10/10 (wt/wt/wt) PA6/PP/ABS Ternary Blends and the Observed Torque Value During Melt-Mixing of the Respective Blends

Code	D_n (μm)	D_w (μm)	Torque (Nm)
8N1P1A	1.46	2.92	2.44
8N1P1A2S	0.43	0.66	3.99
8N1P1A2P	0.49	0.73	3.17
8N1P1A2S2P	0.31	0.62	5.97
8N1P1A1T	1.46	2.83	3.93
8N1P1A2T	1.43	2.77	4.42

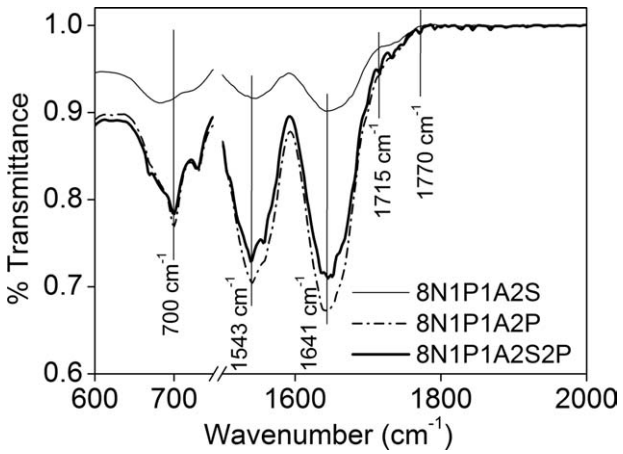

Figure 2. FTIR spectra for 80/10/10 (wt/wt/wt) PA6/PP/ABS ternary blends with compatibilizer.

The formation of "core-shell" type morphology in the present case has been analyzed (the corresponding theoretical analysis[24] is not discussed here) on the basis of spreading coefficient of the respective polymer pairs[15,25] and the theoretical prediction[15] is found to match well with the morphological investigation regarding the development of "core-shell" morphology for various ternary polymer blends considered here.

FTIR spectroscopic analysis has been carried out in order to investigate the melt-interfacial reaction between maleic anhydride (MA) moiety of the compatibilizer and amine (-NH_2) end group of PA6 in 80/10/10 (wt/wt/wt) PA6/PP/ABS ternary blends. Figure 2 depicts the extended spectral region (1500–2000 cm^{-1}) of 80/10/10 (wt/wt/wt) PA6/PP/ABS ternary blends in the presence of compatibilizer. The characteristic peak of PA6 at 1641 cm^{-1} represents carbonyl (C=O) stretching vibration ($\upsilon_{C=O}$), which corresponds to amide I band. The peak at 1543 cm^{-1} can be assigned for amide II band for PA6.[26,27] Peak at 700 cm^{-1} can be assigned due to the out-of-plane deformation vibration of the phenyl ring of styrene (of the ABS phase), which has been considered as an internal standard. The peak at 1770 cm^{-1} in the case of ternary blends involving PP-*g*-MA/SMA or the both clearly shows the formation of imide linkage, which may be due to the reaction between the amine (-NH_2) end group of PA6 and the MA moiety of the compatibilizer. The peak at $\sim$ 1715 cm^{-1} corresponds to carboxylic acid stretch. It is also to be noted that the characteristic peaks for SMA copolymer have been observed at 1782 cm^{-1} and 1859 cm^{-1} corresponding to the MA moiety and PP-*g*-MA shows the characteristic peaks at $\sim$ 1710 cm^{-1} and 1778 cm^{-1} (the corresponding Figures are not shown here). Bhattacharyya et al.[27] have attributed the peaks at 1770 cm^{-1} and at 1702 cm^{-1} to the formation of imide group in composites of PA6 and SMA modified SWNTs. The formation of the imide peaks in PA6-based blends has been addressed in couple of literatures extensively.[28,29] The extent of melt-interfacial reaction may be less even in the presence of 4 wt % compatibilizer due to the simultaneous mixing strategy adopted during melt-mixing. We could earlier observe a complete miscibility between SMA8 and ABS phase and between PP and PP-*g*-MA (as detected by the glass transition temperature, the corresponding result is not shown here). In this context, more experiments need to be carried out systematically to address the localization of the compatibilizer in the ternary polymer blends.

The influence of single and dual compatibilizer and MWNTs on the phase morphology of 80/10/10 (wt/wt/wt) PA6/PP/ABS ternary blends is exhibited in Figure 3. Selective etching of the respective dispersed phases reveals that the "core-shell" type morphology in the corresponding blends remains unaltered in the presence of either compatibilizer or MWNTs. The variation in the average droplet size of the respective dispersed phases is summarized in Table II. Figure 3(a) shows the phase morphology of 80/10/10 (wt/wt/wt) PA6/PP/ABS blends, in the presence of SMA8, which depicts a significant reduction in domain size of the dispersed phase (see Table II). A similar observation is also observed in the presence of PP-*g*-MA [Figure 3(b)] and in the presence of dual compatibilizer [Figure 3(c)]. SMA8 and PP-*g*-MA are expected to act as an efficient compatibilizer in PA6/ABS and PP/ABS binary blends respectively.[30,31] In the present context, the efficiency of the dual compatibilizer in arresting the coalescence process is found to be better as compared to the addition of either SMA8 or PP-*g*-MA as indicated from the morphological refinement (Table II). The extent of compatibilization in the presence of various reactive compatibilizers can also be rationalized from the observed torque data during melt-mixing (Table II). Torque data also indicate a lesser extent of melt-interfacial reaction in the presence of a single compatibilizer (SMA8 or PP-*g*-MA) as compared to the addition of dual compatibilizer in 80/10/10 (wt/wt/wt) PA6/PP/ABS blends, which may be related to the fact that compatibilizer concentration of 2 wt% may not be sufficient for interfacial saturation. Further, it also indicates that both the compatibilizers are engaged in the melt-interfacial reaction which is manifested in higher torque value in case of dual compatibilizer-based ternary blends.

Influence of MWNTs on the phase morphology of 80/10/10 (wt/wt/wt) PA6/PP/ABS ternary blends is depicted in Figure 3(d). The addition of MWNTs does not alter the "core-shell" type of morphology in 80/10/10 (wt/wt/wt) PA6/PP/ABS ternary blends. It is also observed that droplet size of the dispersed phase decreases marginally with increase in MWNTs concentration (Table II). This observation suggests the "compatibilizer-like" action of MWNTs is not evident up to 2 wt % concentration. However, the torque data suggest a progressive increase in the torque value with increase in MWNTs concentration, which indicate an increase in the melt-viscosity of the ternary blends in the presence of MWNTs. The refinement in the dispersed phase of the binary and the ternary blends of PA6/ABS, PP/ABS, and PA6/PP/ABS has earlier been observed with the addition of higher concentration of MWNTs,[26,32,6] which has been understood on the basis of compatibilizer-like action of MWNTs. It has also been realized that a majority fraction of MWNTs localize selectively in one of the phases of these blends, thereby altering the viscosity ratio of the blends. Along with this, MWNTs may also arrest coalescence phenomenon of the droplets by imposing physical barrier (due to the "network-like" structure formation) between the droplets.

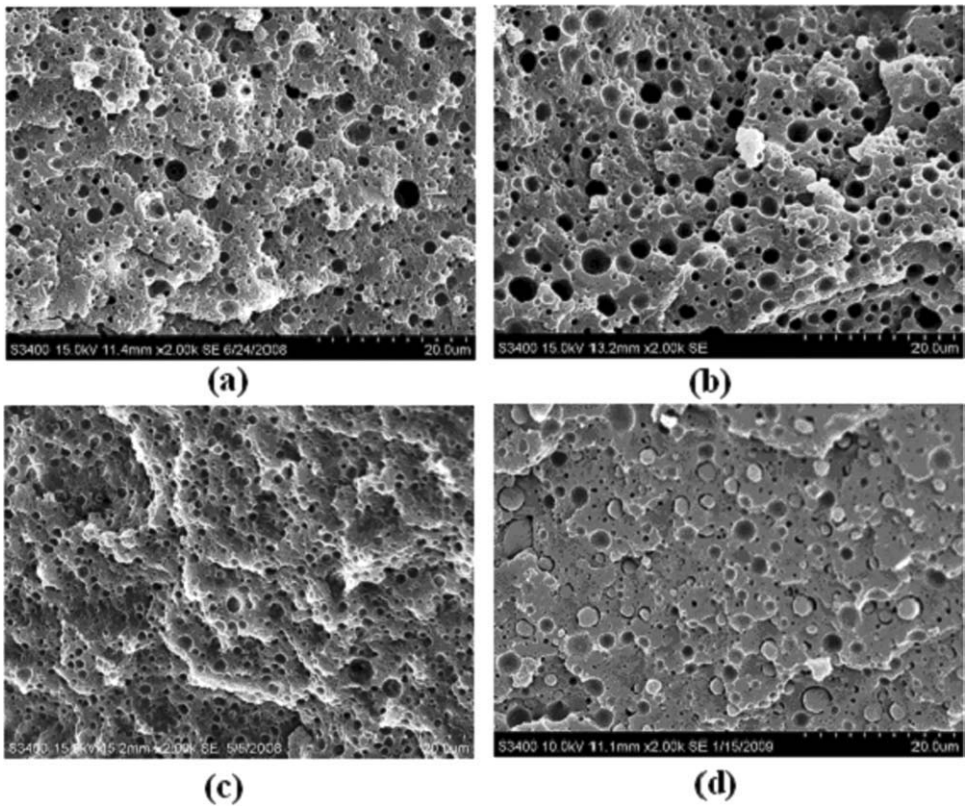

Figure 3. SEM micrographs of cryo-fractured and PP phase etched surface of 80/10/10 (wt/wt/wt) PA6/PP/ABS ternary blends with (a) 2 wt % of SMA8, (b) 2 wt % of PP-*g*-MA, and (c) 4 wt % of (SMA8+ PP-*g*-MA); and (d) ABS phase etched surface of 80/10/10 (wt/wt/wt) PA6/PP/ABS ternary blends with 2 wt % of MWNTs.

Dielectric Relaxation Spectroscopy of 80/10/10 (wt/wt/wt) PA6/PP/ABS Ternary Blends

In order to investigate the effect of blending and the influence of single and dual compatibilizer on the relaxation phenomenon of PA6, dielectric relaxation spectroscopy has been carried out. The variation of dielectric loss modulus (M'') as a function of temperature at a fixed frequency (1 KHz) for pure PA6, 80/10/10 (wt/wt/wt) PA6/PP/ABS blends and compatibilized ternary blends is presented in Figure 4. PA6 exhibits three relaxation peaks; low temperature γ-relaxation, β-relaxation and higher temperature α-relaxation.[17,33–35] Motions of short range -CH_2 segments are responsible for the γ-relaxation, motions of more extended –CH_2 segments and mobile amide groups are responsible for β-relaxation and large-scale motions of chain segments in the vicinity of the glass transition temperature (T_g) are responsible for α-relaxation. In our case, α-relaxation of the PA6 phase could only be detected due to selected narrow temperature range of the measurement. Dielectric properties of PP are unaltered under varying temperature and frequency due to its nonpolar nature.[32] However, Nishikawa et al.[36] have reported that ABS shows α-relaxation peak corresponding to primary relaxation process of SAN at $\sim$ 127°C, which is also not observed in our case as the upper measurement temperature was restricted to 120°C.

Pure PA6 shows a strong peak or α-relaxation near the glass transition temperature ($T_g \sim 50$°C) [Figure 4(a)]. Interestingly,

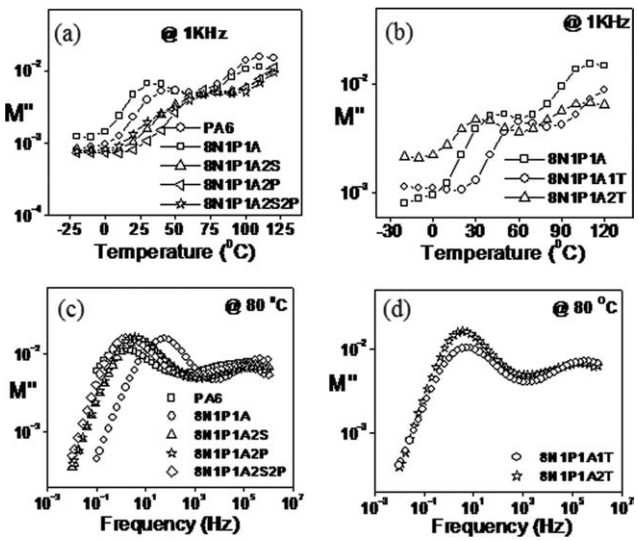

Figure 4. Dielectric loss modulus as a function of temperature at 1 KHz for 80/10/10 (wt/wt/wt) PA6/PP/ABS ternary polymer blends in the presence of (a) compatibilizer and (b) MWNTs; dielectric loss modulus as a function of frequency at 80°C for the respective blends in the presence of (c) compatibilizer and (d) MWNTs.

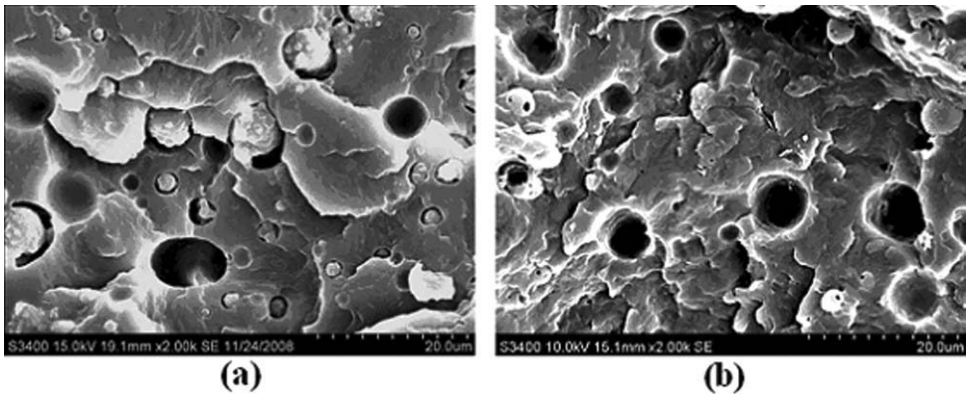

Figure 5. SEM micrographs of cryo-fractured surface of 80/10/10 (wt/wt/wt) PP/PA6/ABS ternary polymer blends (a) etched with THF and (b) etched with formic acid.

α-relaxation peak corresponding to PA6 phase is shifted towards the lower temperature side (∼ 40°C) for 80/10/10 (wt/wt/wt) PA6/PP/ABS ternary blends. The enhanced mobility of the PA6 chain can only be rationalized if the interfacial interaction between the matrix PA6 phase and the "core-shell" dispersed droplets is considered to be less, which otherwise indicates "chain slippage" of PA6 due to the incompatible nature of the blends. Furthermore, α-relaxation peak of PA6 is shifted towards the higher temperature side [Figure 4(a)] for 80/10/10 (wt/wt/wt) PA6/PP/ABS ternary blends in the presence of compatibilizer, which indicates a restriction in PA6 chain mobility due to melt-interfacial reaction in the presence of the compatibilizer. This observation is well supported by the FTIR spectroscopic observation (Figure 2) and also from the observed torque data during melt-mixing as discussed earlier. Interestingly, it is observed from Figure 4(b) that with increase in MWNTs concentration, α-relaxation peak of PA6 is also shifted towards the higher temperature side manifesting the fact that MWNTs may as well hinder the chain mobility of PA6 phase. This observation indicates that a majority of MWNTs may specifically localized in the PA6 phase in 80/10/10 (wt/wt/wt) PA6/PP/ABS ternary blends. The specific localization of a majority fraction of MWNTs in the PA6 phase in 80/10/10 (wt/wt/wt) PA6/PP/ABS blends and in the binary 50/50 (wt/wt) PA6/ABS blends has also been earlier noticed through morphological investigation and also from solution experiment.[6,26]

Figure 4(c) depicts the variation of dielectric loss modulus as a function of frequency for pure PA6 and 80/10/10 (wt/wt/wt) PA6/PP/ABS ternary polymer blends in the presence of compatibilizer at a fixed temperature of 80°C, which is in the range of α-relaxation process of PA6 phase. Pure PA6 (processed under the same processing conditions adopted for ternary polymer blends) exhibits the α-relaxation peak at 7.82 Hz ($\tau = 0.022$ s). PA6 exhibits β-relaxation peak at higher frequency region, i.e., in between $10^5 - 10^6$ Hz along with α-relaxation.[17] α-relaxation peak of PA6 in 80/10/10 (wt/wt/wt) PA6/PP/ABS ternary polymer blends shifts towards the higher frequency side, which may be related to "interfacial slippage" in the uncompatibilized blend as discussed earlier in the text. Addition of either single or dual compatibilizer leads to a shift in α-relaxation peak of PA6 to lower frequency side resulting in higher relaxation time corresponding to PA6 phase. It is observed that PA6 phase shows α-relaxation peak at 3.48 Hz ($\tau = 0.045$ s), 5.21 Hz ($\tau = 0.03$ s), and 2.32 Hz ($\tau = 0.068$ s) corresponding to 80/10/10 (wt/wt/wt) PA6/PP/ABS ternary blends in the presence of SMA8, PP-*g*-MA and dual compatibilizer respectively.

Figure 4(d) shows the variation of dielectric modulus with frequency for 80/10/10 (wt/wt/wt) PA6/PP/ABS ternary polymer blends in the presence of MWNTs at a fixed temperature of 80°C. With increase in MWNTs concentration, α-relaxation peak of PA6 is shifted to the lower frequency side indicating a restriction in PA6 chain mobility provided by MWNTs. It is noticed that PA6 phase exhibits α-relaxation peak at 5.22 Hz ($\tau = 0.03$ s) and 3.48 Hz ($\tau = 0.045$ s) for 80/10/10 (wt/wt/wt) PA6/PP/ABS ternary blends in the presence of 1 and 2 wt % of MWNTs respectively.

The variation in the relaxation time of PA6 phase in various compatibilized blends well correlates with the morphological observation, the observed torque data during melt-mixing and the FTIR spectroscopic analysis. Moreover, the addition of MWNTs in the ternary polymer blends leads to a higher relaxation time of the PA6 phase due to the restriction in PA6 chain mobility, which also supports the observed increase in the torque value during melt-mixing.

Phase Morphology of 80/10/10 (wt/wt/wt) PP/PA6/ABS Ternary Polymer Blends

SEM micrographs of cryo-fractured and etched surfaces of 80/10/10 (wt/wt/wt) PP/PA6/ABS ternary polymer blends are presented in Figure 5. Selective etching of the cryo-fractured surface reveals that ABS phase is involved in the "shell" and PA6 forms "core" in the PP matrix. Morphological analysis shows a wide range of distribution of domain size of PA6 droplets, which indicates the incompatible nature of ternary blends. D_n and D_w of the PA6 droplets in the various ternary blends are reported in Table III.

Figure 6 shows the FTIR spectra for the compatibilized ternary blends of 80/10/10 (wt/wt/wt) PP/PA6/ABS, which exhibit the characteristic absorption peaks of PA6 at 1641 cm^{-1} and 1543 cm^{-1} corresponding to the amide carbonyl groups (as discussed earlier in the text). In the presence of the compatibilizer in the ternary blends, two new peaks are observed at ∼ 1710 cm^{-1}

Table III. Average Droplet Size of PA6 Phase in 80/10/10 (wt/wt/wt) PP/PA6/ABS Ternary Blends and the Observed Torque Value During Melt-Mixing of the Respective Blends

Code	D_n (μm)	D_w (μm)	Torque (Nm)
8P1N1A	2.64	4.21	1.01
8P1N1A2S	2.24	3.39	2.21
8P1N1A2P	1.11	2.89	2.42
8P1N1A2S2P	1.82	3.12	2.59
8P1N1A1T	2.63	4.16	1.05
8P1N1A2T	2.59	3.98	1.21

and at $\sim$ 1780 cm^{-1}, which can be assigned to the unreacted MA moiety of the corresponding PP-*g*-MA and SMA copolymer. The formation of the imide bond in the presence of the compatibilizer could not be detected unequivocally through the FTIR spectroscopy.

Influence of the compatibilizer and MWNTs on the phase morphology of 80/10/10 (wt/wt/wt) PP/PA6/ABS ternary blend is presented in Figure 7. "Core-shell" type morphology is also unaltered in the presence of compatibilizer in this set of blends. A significant reduction in the domain size (see Table III) of the dispersed phase is observed in the presence of compatibilizer.

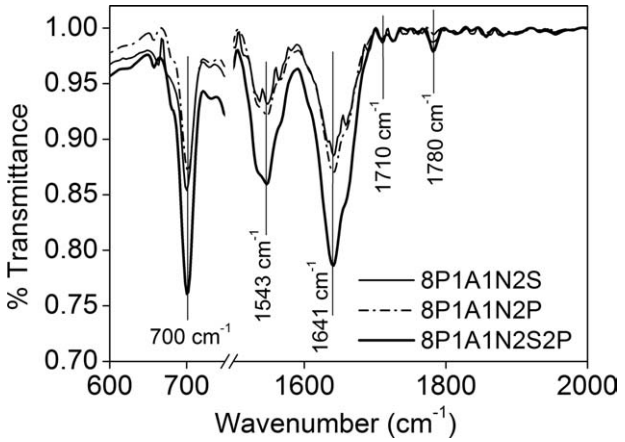

Figure 6. FTIR spectra for 80/10/10 (wt/wt/wt) PP/PA6/ABS ternary blends with compatibilizer.

The reduction in domain size is observed to be higher in the presence of PP-*g*-MA as compared to SMA8 [Figure 7(a, b)]. Interestingly, larger and more elongated domains are found in the presence of dual compatibilizer [Figure 7(c)]. Torque data (shown in Table III) indicate that the extent of melt-interfacial reaction is higher in the presence of dual compatibilizer as compared to the addition of a single compatibilizer.

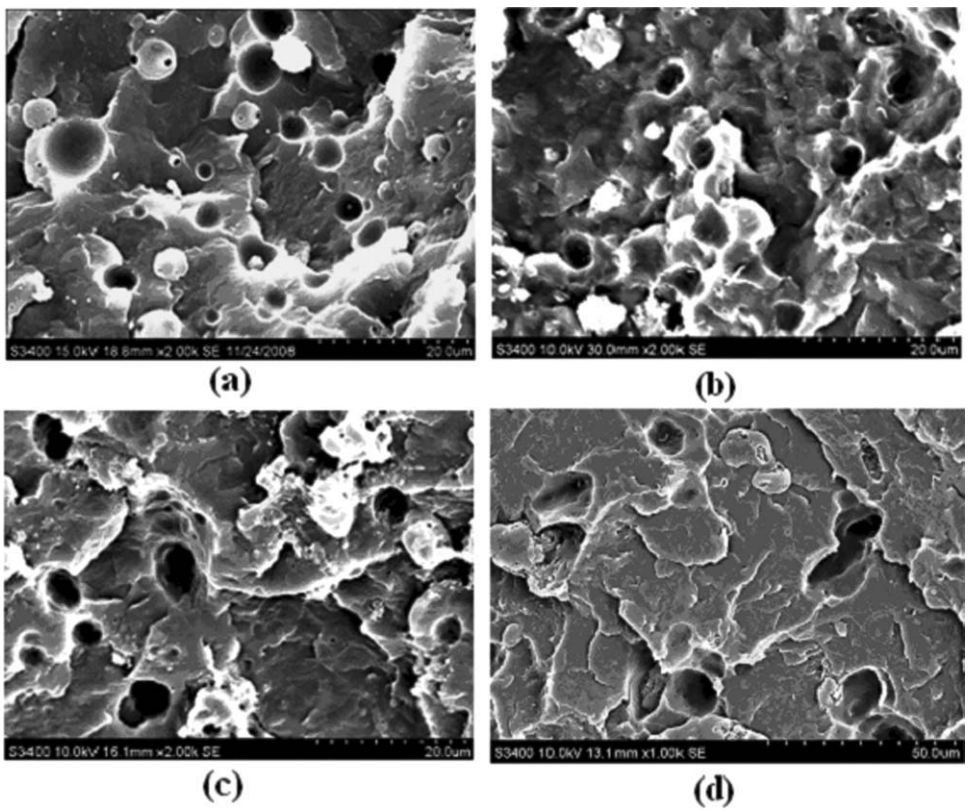

Figure 7. SEM micrographs of cryo-fractured and PA6 phase etched surface of 80/10/10 (wt/wt/wt) PP/PA6/ABS ternary polymer blends with (a) 2 wt % of SMA8, (b) 2 wt % of PP-*g*-MA and (c) 4 wt % of (SMA8+PP-*g*-MA); and (d) PA6 phase etched surfaces of 80/10/10 PP/PA6/ABS ternary blends with 2 wt % of MWNTs.

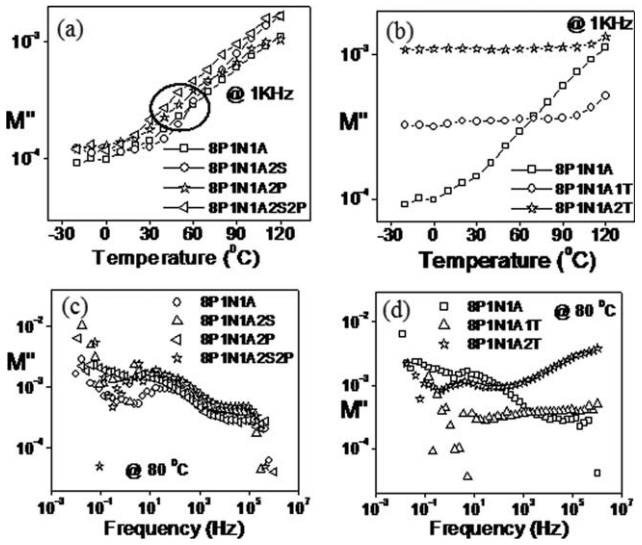

Figure 8. Dielectric loss modulus as a function of temperature at 1 KHz for 80/10/10 (wt/wt/wt) PP/PA6/ABS ternary polymer blends in the presence of (a) compatibilizer and (b) MWNTs; dielectric loss modulus as a function of frequency at 80°C for the respective blends in the presence of (c) compatibilizer and (d) MWNTs.

Figure 7(d) shows that MWNTs do not alter the type of phase morphology of the 80/10/10 (wt/wt/wt) PP/PA6/ABS ternary polymer blends, however, a reduction in the dispersed phase is evident even at low concentration of MWNTs (see Table III). This fact may be attributed to the localization of a majority fraction of MWNTs in the matrix phase (i.e., PP phase), which may alter the viscosity ratio and may also act as a physical barrier which may prevent the coalescence process.[32] However, a fraction of MWNTs also migrates to the PA6 phase as well, which is observed from the morphological observation earlier.[6]

Dielectric Relaxation Spectroscopy of 80/10/10 (wt/wt/wt) PP/PA6/ABS Ternary Polymer Blends

Figure 8(a) exhibits the dielectric loss modulus as a function of temperature for 80/10/10 (wt/wt/wt) PP/PA6/ABS ternary polymer blends in the presence of compatibilizer at a fixed frequency of 1 KHz. Due to nonpolar nature of PP, dielectric properties are almost unaltered with varying temperature and frequency as discussed earlier.[32] α-relaxation peak corresponding to PA6 phase is not very prominent in 80/10/10 (wt/wt/wt) PP/PA6/ABS ternary polymer blends which may be due to high viscous ABS shell (refer Figure 5), which may mask the signature regarding the chain relaxation process associated with the PA6 phase. Moreover, PA6 concentration is also very small as compared to the PP phase. The shift in α-relaxation peak corresponding to PA6 phase is higher in the presence of PP-*g*-MA as compared to SMA8. This fact is well in agreement with the SEM observations [shown in Figure 7(b)], where it is found that the reduction in domain size of the dispersed phase in 80/10/10 (wt/wt/wt) PP/PA6/ABS ternary blends is maximum in the presence of PP-*g*-MA. The higher extent of melt-interfacial reaction in this case may also be rationalized from the observed torque data (Table III) during melt-mixing.

Figure 8(b) shows the variation in dielectric loss modulus (M'') with temperature at a fixed frequency (1 KHz) for 80/10/10 (wt/wt/wt) PP/PA6/ABS ternary blends in the presence of MWNTs. The dielectric loss modulus [Figure 8(b)] is almost independent of temperature for 80/10/10 (wt/wt/wt) PP/PA6/ABS ternary blends in the presence of MWNTs as a majority of MWNTs may be dispersed in the PP phase (the signature associated with the dielectric relaxation for the PP phase is very less), and the localization of a small fraction of MWNTs in the PA6 phase could not enhance the signature associated with the α relaxation due to the small fraction of PA6 content in the blend (mentioned earlier). The state of dispersion of MWNTs in the PP and PA6 phases has been earlier observed through SEM morphological analysis in 80/10/10 (wt/wt/wt) PP/PA6/ABS ternary blends,[6] where the migration of a small fraction of MWNTs from the PP phase to the PA6 phase has been observed.

Figure 8(c) exhibits the dielectric loss modulus as a function of frequency at a fixed temperature of 80°C for 80/10/10 (wt/wt/wt) PP/PA6/ABS ternary blends in the presence of compatibilizer. PA6 phase exhibits α-relaxation peak at 17.60 Hz ($\tau = 0.009$ s) in 80/10/10 (wt/wt/wt) PP/PA6/ABS ternary blends. Further, PA6 phase shows α-relaxation peak at 11.73 Hz ($\tau = 0.013$ s), 7.82 Hz ($\tau = 0.022$ s) and 5.21 Hz ($\tau = 0.031$ s) corresponding to 80/10/10 (wt/wt/wt) PP/PA6/ABS ternary blends in the presence of SMA8, PP-*g*-MA, and dual compatibilizer respectively. Interestingly, the observed shift in α- relaxation peak of PA6 phase is higher in the presence of PP-*g*-MA as compared to SMA8 in 80/10/10 (wt/wt/wt) PP/PA6/ABS ternary blends, manifesting the higher extent of interfacial reaction between amine end groups of PA6 and maleic anhydride moiety of PP-*g*-MA.

The variation of dielectric loss modulus with frequency at a fixed temperature of 80°C for 80/10/10 (wt/wt/wt) PP/PA6/ABS ternary blends with MWNTs is represented in Figure 8(d). PA6 chain relaxes at 13.97 Hz ($\tau = 0.011$ s) in the presence of 1 wt % MWNTs, which is lower as compared to the PA6 phase of 80/10/10 (wt/wt/wt) PP/PA6/ABS ternary blends. The addition of MWNTs shifts α-relaxation peak of PA6 towards the lower frequency side, which indicates the migration of MWNTs from the PP phase to PA6 phase.

The variation in the relaxation time of the PA6 phase in compatibilized 80/10/10 (wt/wt/wt) blends may be in accordance with the melt-interfacial reaction as observed from the increased torque value during melt-mixing. The morphological observation also suggests the better compatibilizing action of PP-*g*-MA as compared to SMA8, due to PP-rich blends. This is in contrast to 80/10/10 (wt/wt/wt) PA6/PP/ABS blends, wherein SMA8 is found to act as a better compatibilizer than PP-*g*-MA. Addition of MWNTs also leads to a restriction of PA6 chain mobility in this blend; however, the corresponding restriction in PA6 chain mobility is much higher in 80/10/10 (wt/wt/wt) PA6/PP/ABS blends in the presence of MWNTs due to the localization of a majority fraction of MWNTs in the PA6 phase.

Phase Morphology of 80/10/10 (wt/wt/wt) ABS/PP/PA6 Ternary Polymer Blends

A separately dispersed phase morphology is observed corresponding to 80/10/10 (wt/wt/wt) ABS/PP/PA6 ternary blends

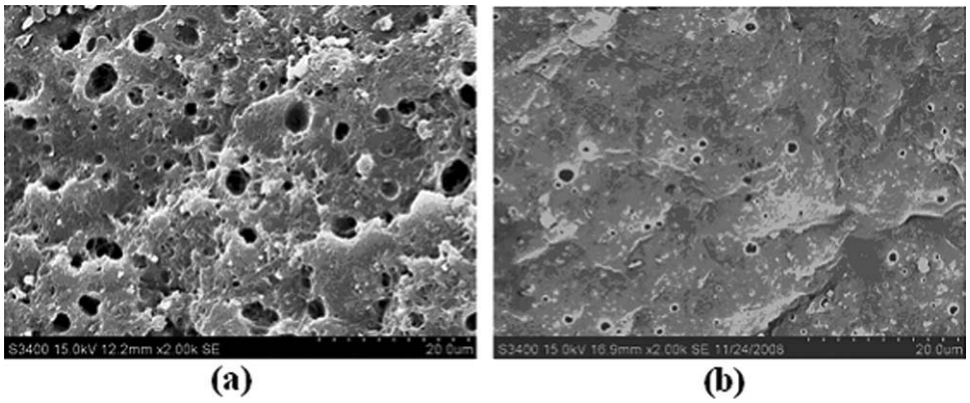

Figure 9. SEM micrographs of cryo-fractured and etched surfaces of 80/10/10 (wt/wt/wt) ABS/PP/PA6 ternary polymer blends (a) etched with formic acid (b) etched with hot xylene.

(Figure 9). Both PA6 and PP phases are dispersed separately in the ABS matrix. Interestingly, it is noticed that the domain size of the PA6 phase is larger than the domain size of the PP phase. Morphological analysis reveals a wide distribution of the dispersed phases. D_n and D_w of the PP and PA6 droplets in the various ternary blends are reported in Tables IV and V.

Figure 10 exhibits the FTIR spectra of 80/10/10 (wt/wt/wt) ABS/PP/PA6 ternary blend in the presence of compatibilizer. The absorption peaks at 1641 cm^{-1}, 1543 cm^{-1} are the characteristic peaks of PA6 phase discussed earlier in the text. In case of compatibilized 80/10/10 (wt/wt/wt) ABS/PP/PA6 ternary blends, new absorption peaks are observed at 1700 cm^{-1} and 1770 cm^{-1}, which supports the formation of imide bond between the MA moiety of compatibilizer and $–NH_2$ end group of PA6 phase.[27]

The phase morphology of compatibilized 80/10/10 (wt/wt/wt) ABS/PP/PA6 ternary polymer blends is shown in Figure 11. In general, a refinement in the dispersed phase has been observed in the presence of a compatibilizer. Addition of dual compatibilizer leads to a transformation of phase morphology from spherically dispersed phase to elongated dispersed phase which may be an indication of coalescence among the finer droplets.[15] Further, torque data (Table V) suggest the higher extent of melt-interfacial reaction in the presence of dual compatibilizer as compared to the addition of a single compatibilizer. The variation in the observed torque value during melt-mixing for these blends is lower as compared to 80/10/10 (wt/wt/wt) PA6/PP/ABS blends. This observation along with morphological investigation suggests a lesser extent of melt-interfacial reaction in this set of blends.

Figure 11(d) represents the SEM micrographs of cryo-fractured and etched surfaces of 80/10/10 (wt/wt/wt) ABS/PP/PA6 ternary blends in the presence of MWNTs. MWNTs do not affect the overall phase morphology of 80/10/10 (wt/wt/wt) ABS/PP/PA6 ternary blends but leads to a reduction in the domain size of the dispersed phases (Tables IV and V).

Dielectric Relaxation Spectroscopy of 80/10/10 (wt/wt/wt) ABS/PP/PA6 Ternary Blends

The variation of dielectric loss modulus with varying temperature at a fixed frequency of 1 KHz for 80/10/10 (wt/wt/wt) ABS/PP/PA6 ternary blends in the presence of compatibilizer is presented in Figure 12(a). α-relaxation peak corresponding to PA6 phase is shifted to the higher temperature side in the presence of compatibilizer, which is consistent with the FTIR spectroscopic analysis and the observed torque data during melt-mixing. Figure 12(b) shows the variation in dielectric loss modulus with temperature at fixed frequency of 1 KHz for 80/10/10 (wt/wt/wt) ABS/PP/PA6 ternary blends with MWNTs. α-relaxation peak corresponding to PA6 phase is slightly shifted towards the higher temperature side, which indicates that a fraction of MWNTs may be localized in the PA6 phase as well (discussed later). It has been earlier observed that MWNTs favor PA6 phase rather than ABS phase due to the lesser surface free energy

Table IV. Average Droplet Size of PP Phase in 80/10/10 (wt/wt/wt) ABS/PP/PA6 Ternary Blends and the Observed Torque Value During Melt-Mixing of the Respective Blends

Code	D_n (μm)	D_w (μm)	Torque (Nm)
8A1P1N	0.57	0.69	3.73
8A1P1N2S	0.48	0.62	4.18
8A1P1N2P	0.32	0.62	4.39
8A1P1N2S2P	0.41	0.58	4.72
8A1P1N1T	0.55	0.69	3.89
8A1P1N2T	0.54	0.68	4.01

Table V. Average Droplet Size of PA6 Phase in 80/10/10 (wt/wt/wt) ABS/PP/PA6 Ternary Blends

Code	D_n (μm)	D_w (μm)
8A1P1N	2.08	2.31
8A1P1N2S	1.44	1.83
8A1P1N2P	1.29	1.66
8A1P1N2S2P	1.38	1.79
8A1P1N1T	1.97	2.12
8A1P1N2T	1.94	2.07

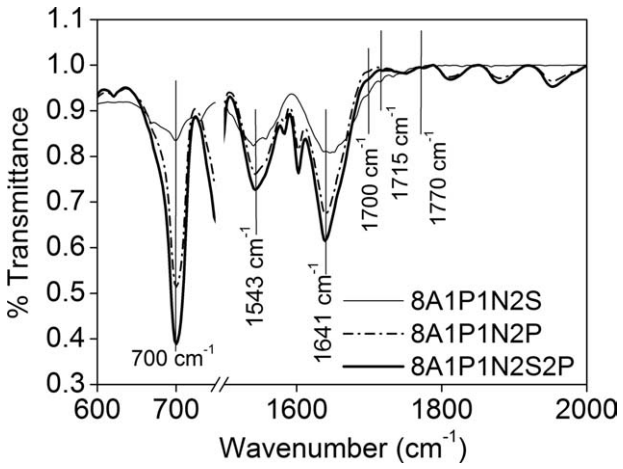

Figure 10. FTIR spectra for 80/10/10 (wt/wt/wt) ABS/PP/PA6 ternary blends with compatibilizer.

difference between PA6 and MWNTs in case of PA6/ABS binary blends.[26] Coupled with this observation, low melt viscosity of the PA6 phase may also favor MWNTs localization. In case of PP/ABS blends, MWNTs were selectively localized in the PP phase due to the low melt-viscosity of the PP phase as compared to the ABS phase,[32] however, the surface free energy difference was found to be lesser between ABS and the MWNTs. In this context, MWNTs are either well dispersed in at the PA6 phase (in the PA6-based blends) or migrated from the other phases to the PA6 phase in the ternary blends (PP/ABS-based blends) during melt-mixing, which may be due to the lower surface energy difference (discussed earlier). Next to the affinity towards the PA6 phase, MWNTs are also dispersed well in the PP phase. However, a majority of MWNTs has redistributed to PA6 and PP phases, in case of ABS-based ternary blends during the addition of the minor phases.[6]

Figure 12(c) shows the variation of dielectric loss modulus with frequency at a fixed temperature of 80°C for 80/10/10 ABS/PP/PA6 ternary polymer blends in the presence of compatibilizer. α-relaxation peak corresponding to PA6 phase is shifted towards the lower frequency side in the presence of compatibilizer. PA6 chain shows α-relaxation peak at 59.4 Hz ($\tau = 0.002$ s) in the presence of PP-*g*-MA, whereas in the presence of dual compatibilizer, the α-relaxation peak appears at 26.4 Hz ($\tau = 0.006$ s).

Figure 12(d) shows the variation in dielectric loss modulus with frequency at fixed temperature of 80°C for 80/10/10 (wt/wt/wt) ABS/PP/PA6 ternary blends in the presence of MWNTs. PA6 phase shows α- relaxation peak at ~ 133.66 Hz ($\tau = 0.001$ s) in 80/10/10 (wt/wt/wt) ABS/PP/PA6 ternary blends which is shifted to ~ 11.73 Hz ($\tau = 0.013$ s) in the presence of 1 wt % MWNTs, manifesting the localization of a fraction of MWNTs in the PA6 phase.

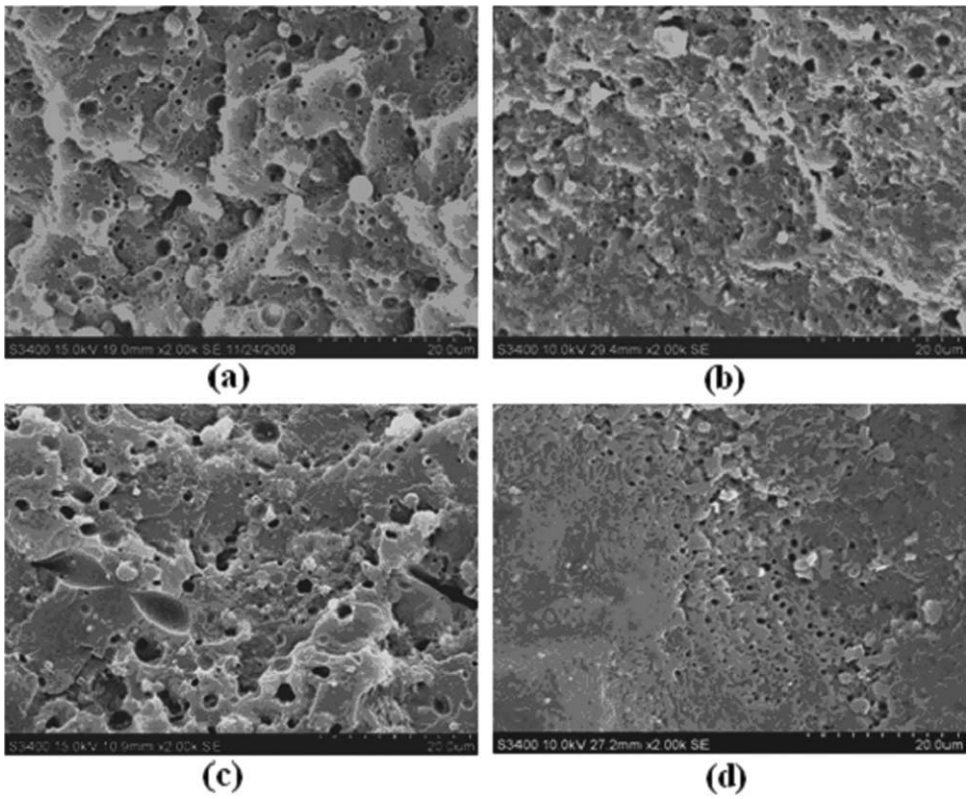

Figure 11. SEM micrographs of cryo-fractured and PP phase-etched surface of 80/10/10 (wt/wt/wt) ABS/PP/PA6 ternary polymer blends with (a) 2 wt % of SMA8, (b) 2 wt % of PP-*g*-MA, and (c) 4 wt % of (SMA8+ PP-*g*-MA); and (d) PP phase etched surfaces of 80/10/10 (wt/wt/wt) ABS/PP/PA6 ternary blends with 2 wt % of MWNTs.

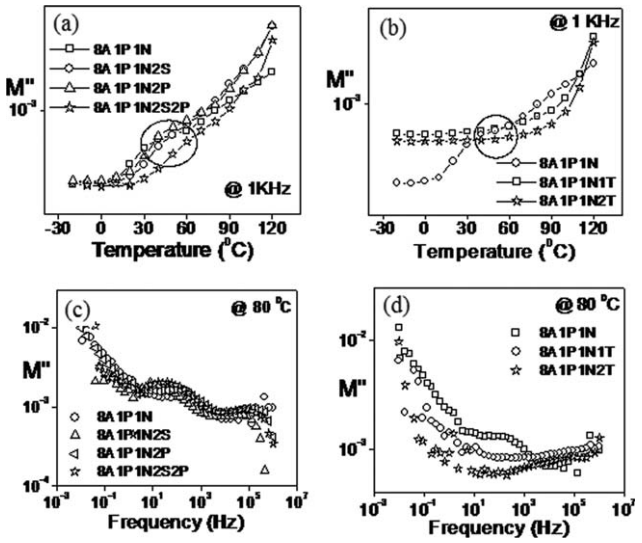

Figure 12. Dielectric loss modulus as a function of temperature at 1 KHz for 80/10/10 (wt/wt/wt) ABS/PP/PA6 ternary polymer blends in the presence of (a) compatibilizer and (b) MWNTs; dielectric loss modulus as a function of frequency at 80°C for the respective blends in the presence of (c) compatibilizer and (d) MWNTs.

The addition of compatibilizer leads to a refinement in the dispersed droplets of 80/10/10 (wt/wt/wt) ABS/PP/PA6 ternary blends due to the melt-interfacial reaction, which is supported by the observed torque data during melt-mixing and also through the observed higher relaxation time corresponding to the PA6 phase. The addition of MWNTs in this blend also shows a similar variation in the relaxation time of the PA6 phase and also in the variation in the torque data during melt-mixing.

DISCUSSION

80/10/10 (wt/wt/wt) PA6/PP/ABS and PP/PA6/ABS ternary blends show "core-shell" type morphology, whereas 80/10/10 (wt/wt/wt) ABS/PP/PA6 ternary blends show "separately dispersed" phase morphology. Addition of compatibilizer or MWNTs does not change the type of phase morphology of the ternary blend in these set of blends. The relaxation time of PA6 chain is significantly affected in various ternary blends as compared to pure PA6, which indicates the enhanced mobility of PA6 chain in the ternary uncompatibilized blends irrespective of whether PA6 involves as a "matrix" or as a "dispersed phase". This observation suggests a highly incompatible nature of the ternary polymer blend which is arising due to "chain slippage" and manifests in lower relaxation time. Morphological observation also indicates a coarse morphology with wider domain size distribution in these ternary blends.

It is also observed (Table VI) that the relaxation time of PA6 chain decreases in the presence of a compatibilizer, the variation in the relaxation time depends on the efficiency of the compatibilizer or otherwise the extent of melt-interfacial reaction dictates the mobility of the PA6 chain. This observation is consistent with 80/10/10 (wt/wt/wt) PA6/PP/ABS, 80/10/10 (wt/wt/wt) PP/PA6/ABS, and 80/10/10 (wt/wt/wt) ABS/PP/PA6 ternary blends in which PA6 phase either involves as a "matrix" or as a "core" or as a "separately dispersed" domain, respectively. The variation in the relaxation time (τ) for the PA6 phase in the presence of MWNTs in the respective ternary blends also follows a similar trend; however, the extent of restriction in the PA6 chain mobility (as observed from the τ values) in the presence of MWNTs depends whether a majority fraction of MWNTs has restricted in the PA6 phase or partially distributed to other phases as well. It is also to be noted that τ for PA6 in 80/10/10 (wt/wt/wt) PA6/PP/ABS blend is significantly higher in the presence of either compatibilizer or MWNTs as compared to τ for PA6 in the corresponding blends of 80/10/10 (wt/wt/wt) PP/PA6/ABS and 80/10/10 (wt/wt/wt) ABS/PP/PA6. This observation clearly indicates that PA6 chains are more restricted when PA6 exhibits as a "matrix" as compared to either as a "core" (in the PP phase) or as a "separately dispersed" domain in the ABS matrix; the issue would be addressed in detail in future.

The extent of melt-interfacial reaction may be higher in 80/10/10 (wt/wt/wt) PA6/PP/ABS blend system as PA6 chain may possibly diffuse more easily to engage in the melt-interfacial reaction. This has resulted in higher normalized torque value (Table VI) with finer average domain size of the dispersed droplets and can be correlated well with the relaxation time of PA6 phase in the corresponding blends.

In contrast, the extent of melt-interfacial reaction may be less in the case of 80/10/10 (wt/wt/wt) ABS/PP/PA6 blends due to the difficulty of PA6 chains to diffuse (which is also in a minor fraction, 10 wt %) in the high viscous ABS matrix to engage in the melt-interfacial reaction with the compatibilizer. This may clearly be observed in the variation of the average droplet size

Table VI. Relaxation Time for the PA6 Phase at a Fixed Temperature of 80°C for the Respective Ternary Blends and Normalized Torque Value During Melt-Mixing

Sample code	Relaxation time, τ (s)	Normalized torque
PA6	0.022	-
8N1P1A	0.002	1.00
8N1P1A2S	0.045	1.63
8N1P1A2P	0.03	1.29
8N1P1A2S2P	0.068	2.44
8N1P1A1T	0.03	1.61
8P1N1A	0.009	1.00
8P1N1A 2S	0.013	2.18
8P1N1A 2P	0.022	2.39
8P1N1A2S2P	0.031	2.56
8P1N1A1T	0.011	1.03
8A1P1N	0.001	1.00
8A1P1N2S	0.002	1.12
8A1P1N2P	0.002	1.17
8A1P1N2S2P	0.006	1.26
8A1P1N1T	0.013	1.04

of the dispersed phases and in the normalized torque values (Table VI) during melt-mixing. The observed higher relaxation time of PA6 chains in these compositions corresponds well with the morphological observation.

Further, normalized torque values (Table VI) also indicated a higher extent of melt-interfacial reaction in 80/10/10 (wt/wt/wt) PP/PA6/ABS blends. The corresponding relaxation time of PA6 phase is also well in agreement with the normalized torque value, even if PA6 forms "core" and surrounded by ABS 'shell' in the PP matrix. It is also expected that melt-interfacial reaction may possibly occur even before the development of "core-shell" morphology. On the contrary, the observed average domain size of the dispersed phase (PA) indicated a lesser extent of melt-interfacial reaction in the presence of compatibilizer as compared to 80/10/10 (wt/wt/wt) PA6/PP/ABS blend. This has been resulted in higher relaxation time of the PA6 chain in 80/10/10 (wt/wt/wt) PP/PA6/ABS blend as compared to 80/10/10 (wt/wt/wt) ABS/PP/PA6 blend, however, lower than 80/10/10 (wt/wt/wt) PA6/PP/ABS blend.

The variation in the relaxation time of the PA6 chain in the presence of MWNTs in various ternary blends also follows a similar trend (Table VI). However, the localization of MWNTs preferentially to the PA6 phase or partially migrated to the other phases may possibly determine the extent of mobility of the PA6 chains in the corresponding blends.

SUMMARY AND CONCLUSIONS

Ternary polymer blends of PA6, PP, and ABS were prepared in the presence of compatibilizer or MWNTs by melt-mixing in order to investigate the influence of compatibilizer and MWNTs on the phase morphology and dielectric relaxation behavior of the PA6 phase in the respective ternary polymer blends. Morphological analysis showed the 'core-shell' type morphology in the ternary polymer blends of 80/10/10 (wt/wt/wt) PA6/PP/ABS and 80/10/10 (wt/wt/wt) PP/PA6/ABS. 80/10/10 (wt/wt/wt) ABS/PP/PA6 ternary blends exhibited "separately dispersed" phase morphology. The type of phase morphology was unaltered in the presence of either compatibilizer or MWNTs. However, morphological refinement was observed in the presence of either compatibilizer or MWNTs in the respective ternary blend which was either due to the melt-interfacial reaction between the $-NH_2$ end group of PA6 and MA moiety of the compatibilizer or alteration of viscosity ratio due to the localization of MWNTs in the corresponding phase/s.

Dynamic relaxation spectroscopic analysis indicated an increase in the relaxation time of PA6 chain in the presence of compatibilizer in the respective ternary blend. The variation in the relaxation time was dependent on the efficiency of the compatibilizer. The variation in the relaxation time for PA6 in the presence of MWNTs in the respective ternary blends also followed a similar trend; however, the extent of restriction depends on whether MWNTs are localized 'solely' in the PA6 phase or partially distributed to other phases as well.

Overall, the influence of compatibilizer and MWNTs on the phase morphology has been investigated in the ternary polymer blends of PA6, PP, and ABS. Dielectric relaxation spectroscopic analysis revealed the influence of blend composition and the addition of either compatibilizer or MWNTs on the chain mobility of the PA6 phase.

ACKNOWLEDGMENTS

The authors duly acknowledge "Microcompouder Central facility," IIT Bombay and one of the authors (BP) would like to acknowledge Mr. Dileep Agrahari for extending his co-operation during DRS measurements. One of the authors (ARB) would like to acknowledge the financial support from the Department of Science and Technology (DST), India (Project No. 08DST016).

REFERENCES

1. Paul, D. R. Polymer Blends (vols. 1 and 2); Academic Press: San Diego, CA, **1978.**
2. Olabisi, O.; Robeson, L. M.; Shaw, M. T. Polymer–Polymer Miscibility; Academic Press: San Diego, CA, **1979.**
3. Nishi, T.; Akiyam, S.; Inoue, T. Polymer Blends; CMC Press: Tokyo, **1981.**
4. Bhattacharyya, A. R.; Ghosh, A. K.; Misra, A. Polymer **2003,** *44*, 1725.
5. Panda, B.; Bhattacharyya, A. R.; Kulkarni, A. R. *American Chemical Society, PMSE Division, Polym. Prepr.* **2009,** *101*, 894.
6. Panda, B.; Bhattacharyya, A. R.; Kulkarni, A. R. *Polym. Eng. Sci* **2011,** *51*, 1550.
7. Hobbs, S. Y.; Dekkers, M. E. *J.; Watkins, V. H. Polymer* **1998,** *29*, 1598.
8. Favis, B. D.; Chalifoux, J. P. *Polymer* **1988,** *29*, 1761.
9. Reignier, J.; Favis, B. D.; Heuzey, M. C. *Polymer* **2003,** *44*, 49.
10. Reignier, J.; Favis, B. D. *Macromolecules* **2000,** *33*, 6998.
11. Bhattacharyya, A. R.; Ghosh, A. K.; Misra, A. *Polymer* **2001,** *42*, 9143.
12. Xanthos, M. *Polym. Eng. Sci.* **1988,** *28*, 1392.
13. Ha, C. S.; Park, H. D.; Cho, W. J.J. *Appl. Polym. Sci.* **2000,** *76*, 1048.
14. Fang, Z. P.; Zeng, M. F.; Cai, G. P.; Xu, C. W. *J. Appl. Polym. Sci.* **2001,** *82*, 2947.
15. Omonov, T. S.; Harrats, C.; Groeninckx, G. *Polymer* **2005,** *46*, 12322.
16. Wang, D.; Xie, X. M. *Polymer* **2006,** *47*, 7859.
17. Urman, K.; Madhouly, S.; Otaigbe, J. U. *Polymer* **2007,** *48*, 1659.
18. Fuse, N.; Sato, H.; Ohki, Y.; Tanaka, T. *IEEE Trans. Dielectrics Electrical Insulation* **2009,** *16*, 524.
19. Logakis, E.; Pandis, C.; Peoglos, V.; Pissis, P.; Pionteck, J.; Pötschke, P.; Mičušık, M.; Omastová, M. *Polymer* **2009,** *50*, 5103.
20. Laredo, E.; Grimau, M.; Bello, A.; Sánchez, F.; Gómez, M. A.; Marco, C.; Campy, I.; Arribas, J. M. *J. Polym. Sci.: Part B* **2005,** *43*, 1408.
21. George, S.; Varughese, K. T.; Thomas, S. J. *Appl. Polym. Sci.* **1999,** *73*, 255.

22. Hassan, M. K.; Wiggins, J. S.; Storey, R. F.; Mauritz, K. A. *Polymer* **2007,** *48*, 2022.
23. Valera, T. S.; Augusto, T. M.; Nicole, R. D. *Macromolecules* **2006,** *39*, 2663.
24. . Ph.D. Thesis, Biswajit Panda, Indian Institute of Technology Bombay, **2011.**
25. Wu, S. Polymer Interface and Adhesion; Marcel Dekker: New York, **1982.**
26. Bose, S; Bhattacharyya, A. R.; Kulkarni, A. R.; Pötschke, P. *Compos. Sci. Technol.* **2009,** *69*, 365.
27. Bhattacharyya, A. R.; Pötschke, P.; Häußler, L.; Fischer, D. *Macromol. Chem. Phys.* **2005,** *206*, 2084.
28. Schäfer, R.; Kressler, J.; Neuber, R.; Mülhaupt, R. *Macromolecules* **1985,** *28*, 5037.
29. Eichhorn, K.-J.; Lehmann, D.; Voigt, D. J. *Appl. Polym. Sci.* **1996,** *62*, 2053.
30. Bose, S.; Bhattacharyya, A. R.; Kodgire, P. V.; Misra, A. *Polymer* **2007,** *48*, 356.
31. Khare, R. A.; Bhattacharyya, A. R.; Kulkarni, A. R. *J. Appl. Polym. Sci.* **2011,** *120*, 2663.
32. Khare, R. A.; Bhattacharyya, A. R.; Kulkarni, A. R.; Saroop, M.; Biswas, A. J. *Polym. Sci. Part B* **2008,** *46*, 2286.
33. Frank, B.; Frubing, P.; Pissis, P. J. *Polym. Sci. Part B* **1996,** *34*, 1853.
34. Laredo, E.; Grimau, M.; Sanchez, F.; Bello, A. *Macromolecules* **2003,** *36*, 9840.
35. Laredo, E.; Hernandez, M. C. *J. Polym. Sci. Part B* **1997,** *35*, 2879.
36. Nishikawa, K.; Hirosh, Y.; Urakawa, O.; Adachi, K.; Hatano, A.; Aoki, Y. *Polymer* **2002,** *43*, 1483.
37. Kessairi, K.; Napolitano, S.; Capaccioli, S.; Rolla, P.; Wübbenhorst, M. *Macromolecules* **2007,** *40*, 1786.